Duncan et al., Supplementary Fig. 1

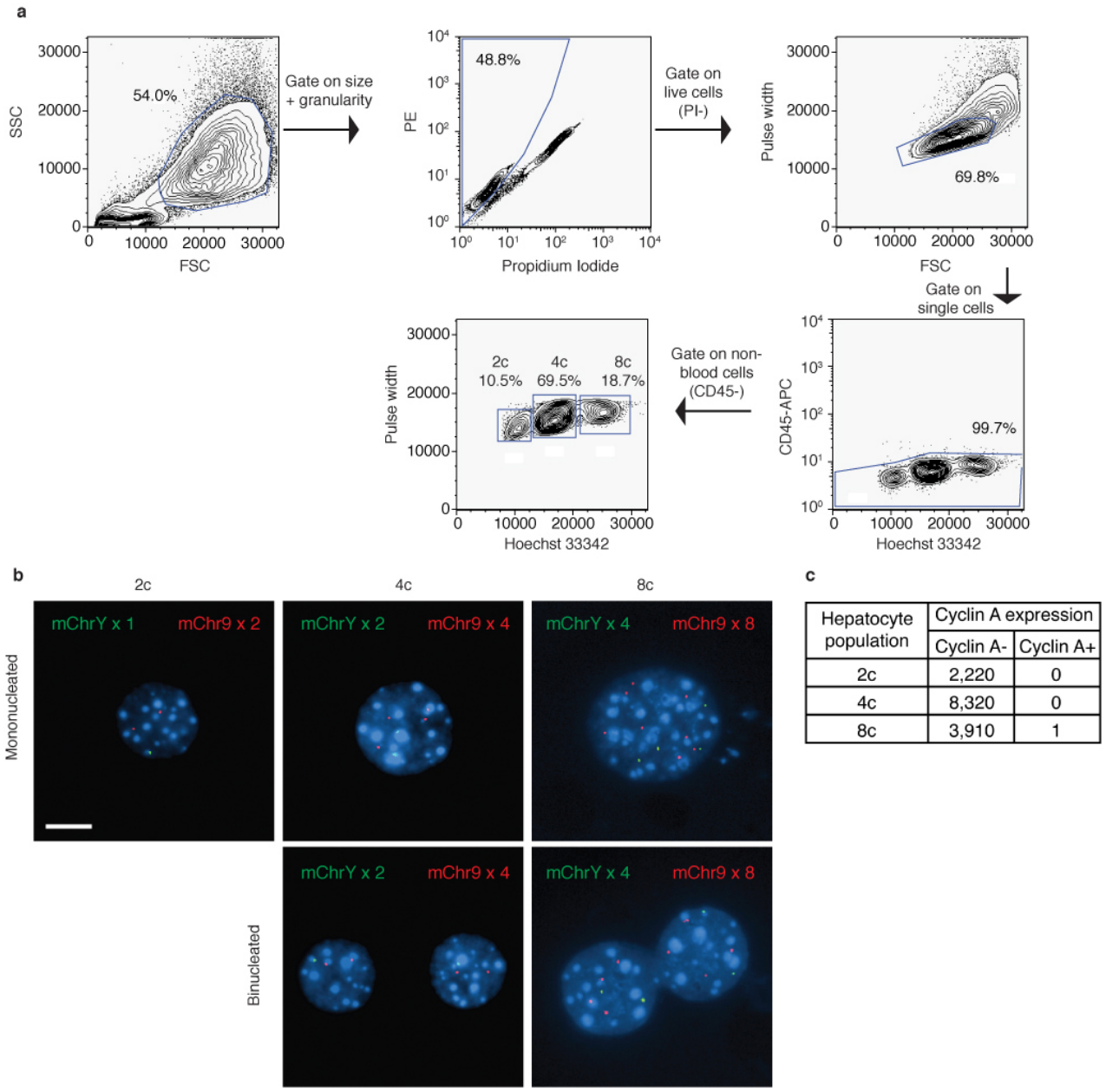

c

Hepatocyte population	Cyclin A expression	
	Cyclin A-	Cyclin A+
2c	2,220	0
4c	8,320	0
8c	3,910	1

FACS-isolated 8c hepatocytes are highly pure. a, Gating strategy for identifying hepatocyte populations based on DNA content. **b,** Detection of mChrY and mChr9 by FISH. FACS-isolated hepatocytes from male mice were hybridized with fluorescent labeled BAC probes against mChrY (green) and mChr9 (red). >99% of hepatocytes contained the expected number of FISH signals. Diploid hepatocytes contained a single nucleus (mChrY x 1 and mChr9 x 2). Tetraploid hepatocytes were either mononucleated (mChrY x 2 and mChr9 x 4) or binucleated (with each nucleus containing mChrY x 1 and mChr9 x 2). Octaploid hepatocytes were either mononucleated (mChrY x 4 and mChr9 x 8) or binucleated (with each nucleus containing mChrY x 2 and mChr9 x 4). Scale bar is 10 µm. **c,** Purified hepatocytes from wild-type mice (aged 5-6 months; *n*=3) were stained with Cyclin A, which is highly expressed in S/G2 phases of the cell cycle. The number of Cyclin A positive and negative cells is shown. Together, the FISH and Cyclin A data indicated the majority (>99%) of sorted octaploid hepatocytes were indeed 8n8c and not 4n8c.

Duncan et al., Supplementary Fig. 2

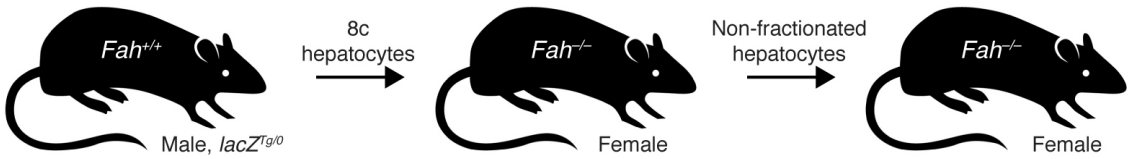

Transplantation scheme for *in vivo* expansion of purified octaploid hepatocytes. 8c hepatocytes isolated from 3-6 month old male mice (hemizygous for Rosa26 *lacZ*) were transplanted into female *Fah*$^{-/-}$ recipient mice. After repopulation, non-fractionated hepatocytes were serially transplanted into secondary *Fah*$^{-/-}$ female recipients. Highly pure octaploid hepatocytes were used in transplantation assays for several reasons. First, contamination during fluorescence-activated cell sorting (FACS) with diploid hepatocytes is less likely than with tetraploid cells. Secondly, tetraploids in the G2 phase of the cell cycle (4n8c) cannot explain the emergence of diploid mitotic products. Finally, if an octaploid cell simply completed cytokinesis, it could potentially generate 2 tetraploids but never produce a diploid. Thus, emergence of diploid cells from an octaploid precursor must be due to ploidy reversal.

Duncan et al., Supplementary Fig. 3

a

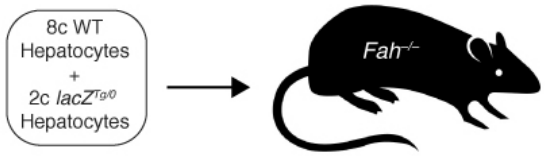

Transplant #	Input: 8c WT (%)	Input: 2c ß-gal+ (%)	Output: Normalized ß-gal+ (%)	ß-gal ratio (output/ input)
1	99	1	0.7	0.7
2	90	10	16	1.6
3	80	20	22	1.1
4	75	25	28	1.1
average ± SEM				1.1 ± 0.2

b

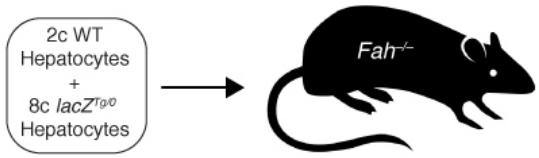

Transplant #	Input: 2c WT (%)	Input: 8c ß-gal+ (%)	Output: Normalized ß-gal+ (%)	ß-gal ratio (output/ input)
1	95	5	4	0.8
2	90	10	12	1.2
3	90	10	9	0.9
average ± SEM				1.0 ± 0.1

Octaploid and diploid hepatocytes share equivalent repopulation potential. a, Purified 8c hepatocytes (from wild-type mice) were mixed with limiting numbers of purified 2c hepatocytes (from FAH+ mice hemizygous for *lacZ*) and transplanted into *Fah*$^{-/-}$ recipient mice. The percentage of each transplanted population is indicated. Hepatocytes were isolated from repopulated livers, and the frequency of donor-derived cells determined (i.e., % FAH+ and % ß-gal+). The percentage of ß-gal+ cells was normalized across all experiments by the following equation: [% ß-gal+] / [% FAH+] x 100. Expansion of 2c cells (ß-gal+) was calculated as follows: [% normalized ß-gal+ after repopulation] / [% ß-gal+ cells originally transplanted]. Relative to 8c transplanted hepatocytes, 2c hepatocytes expanded 1.1 ± 0.2-fold (*n*=4 mice). **b,** The opposite experiment was also performed. Limiting numbers of 8c hepatocytes (from FAH+ mice hemizygous for *lacZ*) were co-transplanted with 2c hepatocytes (from wild-type mice). The degree of expansion by 8c hepatocytes (ß-gal+) was calculated in repopulated mice. Relative to 2c hepatocytes, 8c hepatocytes expanded 1.0 ± 0.1-fold (*n*=3 mice). Together, these results indicate that 2c and 8c hepatocytes proliferate equivalently *in vivo.*

Duncan et al., Supplementary Fig. 4

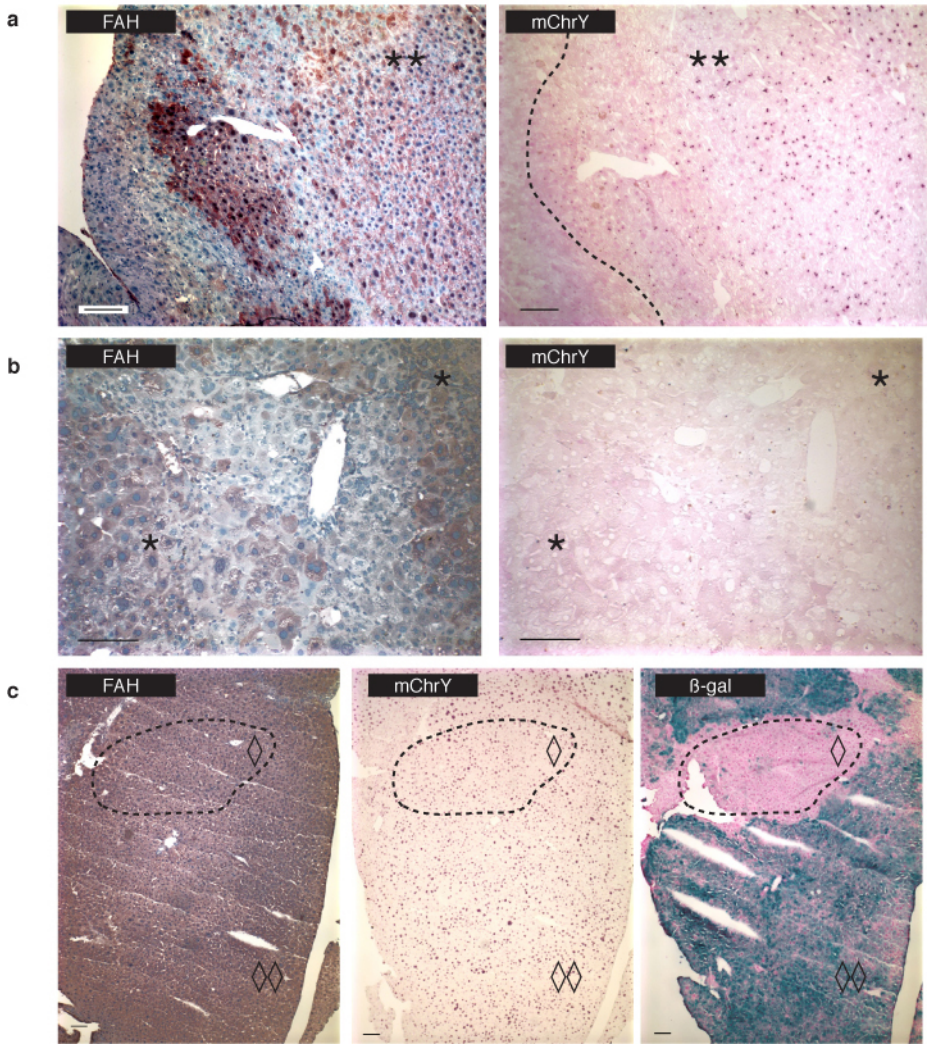

Marker loss in hepatocytes derived from octaploid hepatocytes. Marker analysis on sequential liver sections from primary transplanted mice described in Supplementary Fig. 1a (*n*=3-6). FAH+ nodules (brown) either contained signal mChrY staining (**a**) or lacked mChrY staining (**b**). Double asterisks (**) indicate double positive nodules (FAH+ and mChrY+) whereas single asterisks (*) indicate single positive nodules (FAH+ and mChrY-). ß-gal activity (blue) co-localizes with most, but not all nodules expressing FAH and mChrY (**c**). Double diamonds (◊◊) indicate nodules expressing all donor markers (FAH+, mChrY+ and ß-gal+) and single diamonds (◊) indicate marker loss (Fah+, mChrY+ and ß-gal-). Scale bars are 400 μm.

Duncan et al., Supplementary Fig. 5

a

Young mice *n*=3		Adult mice *n*=5		Aged mice *n*=6	
Age	Sex	Age	Sex	Age	Sex
20d	M	4 mo	F	10 mo	M
21d	M	4 mo	M	11 mo	F
21d	M	4 mo	M	12 mo	M
		5 mo	M	12 mo	F
		5 mo	F	14 mo	F
				15 mo	M

b

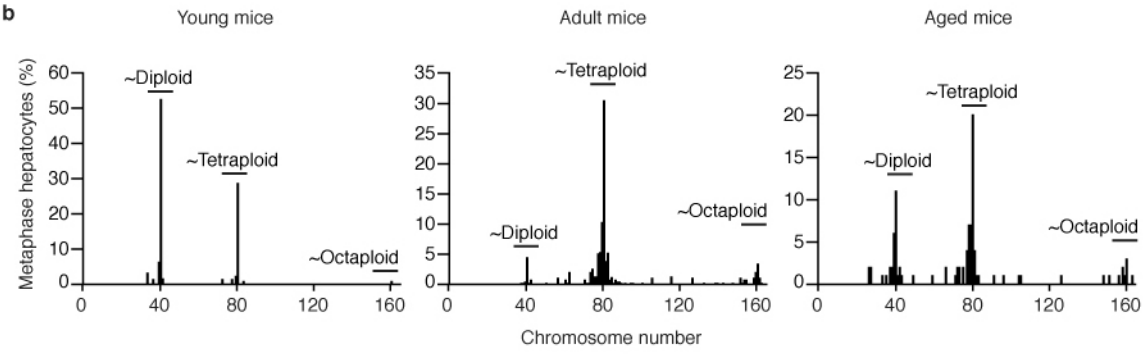

c

	Nearest ploidy	Number	Gains	Losses
Young mice	*Diploid*	39	None	2
		40	2	12
		42	4, 6, 9	16
	Tetraploid	76	None	1, 2, 15, 16
		77	14	11, 6, 18, Y
		80	2	7
Adult mice	*Diploid*	41	4, 5, 6x2, 11, 16	7, 14, 15, 18, 19
	Tetraploid	70	11	2, 5x2, 7, 10, 12, 15x2, 16, 19x2
		78	None	7, 10
		81	19	None
		83	4, 14, Y	None
	Octaploid	153	8	2, 6, 9, 11, 14x3, 16
Aged mice	*Tetraploid*	79	5, 9	3, 13, Y
		80	3, 6	7, 8
		81	3, 12	16
	Octaploid	158	14, 15, 16, 19x2	2, 6, 8x3, 11, 17
		159	6, 11, 12, 15, 16, 17, 19	3x2, 4, 5, 7x3, Y
		160	8, 16, 17, 18, 19	7, 11x2, 12, 15

Aneuploidy in hepatocytes from wild-type mice. Cytogenetic analysis was performed on hepatocytes isolated from wild-type, non-transplanted mice. **a,** Three age groups were analyzed. Multiple strains were used, including C57Bl, 129, BalbC and F1 hybrid (C57Bl x SJL). **b,** Chromosome number is shown for each age group. **c,** Representative aneuploid karyotypes (chromosomal gains/losses) are also shown. Chromosomal rearrangements were rarely detected. Chromosomal gains and losses are described relative to the nearest ploidy level.

Multiple controls were included in the cytogenetic analysis of hepatocytes from wild-type mice. First, studies were performed on both male and female animals from different strain backgrounds. Secondly, to control for an undiagnosed infection in our colony, two adult mice analyzed were imported from The Jackson Laboratories and hepatocytes analyzed immediately upon arrival. Finally, problems with cytogenetic technique could be excluded because peritoneal fibroblasts (data not shown) from the analyzed mice consistently produced normal karyotypes.

Duncan et al., Supplementary Fig. 6

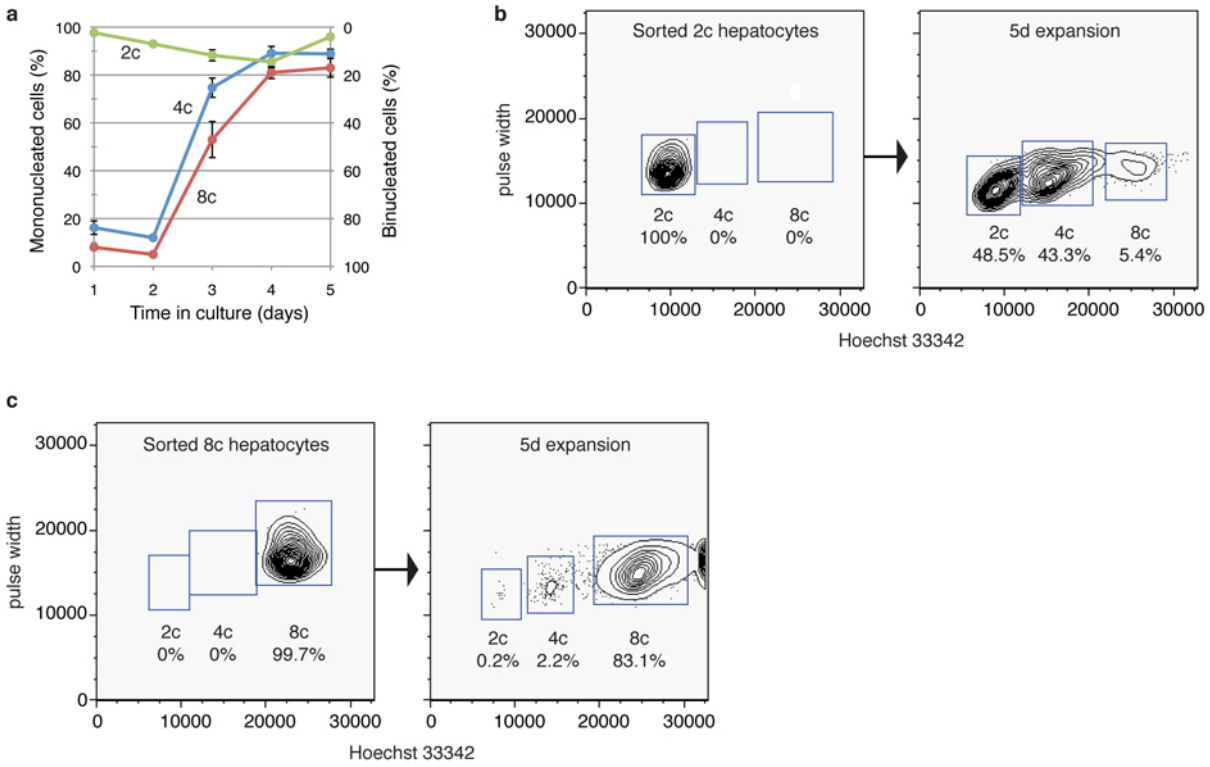

Expansion of hepatocyte populations *in vitro*. a, Freshly-isolated 4c and 8c hepatocytes were predominately binucleated, and they became increasingly mononucleated over time. In contrast, 2c hepatocytes were exclusively mononucleated, and 10-20% became binucleated. Data points represent average values ± s.e.m. (*n*=6-10). **b, c,** DNA content of cultured 2c and 8c hepatocytes was determined by flow cytometry. Representative FACS plots are shown for freshly-sorted hepatocyte populations and cells expanded for 5d.

Duncan et al., Supplementary Fig. 7

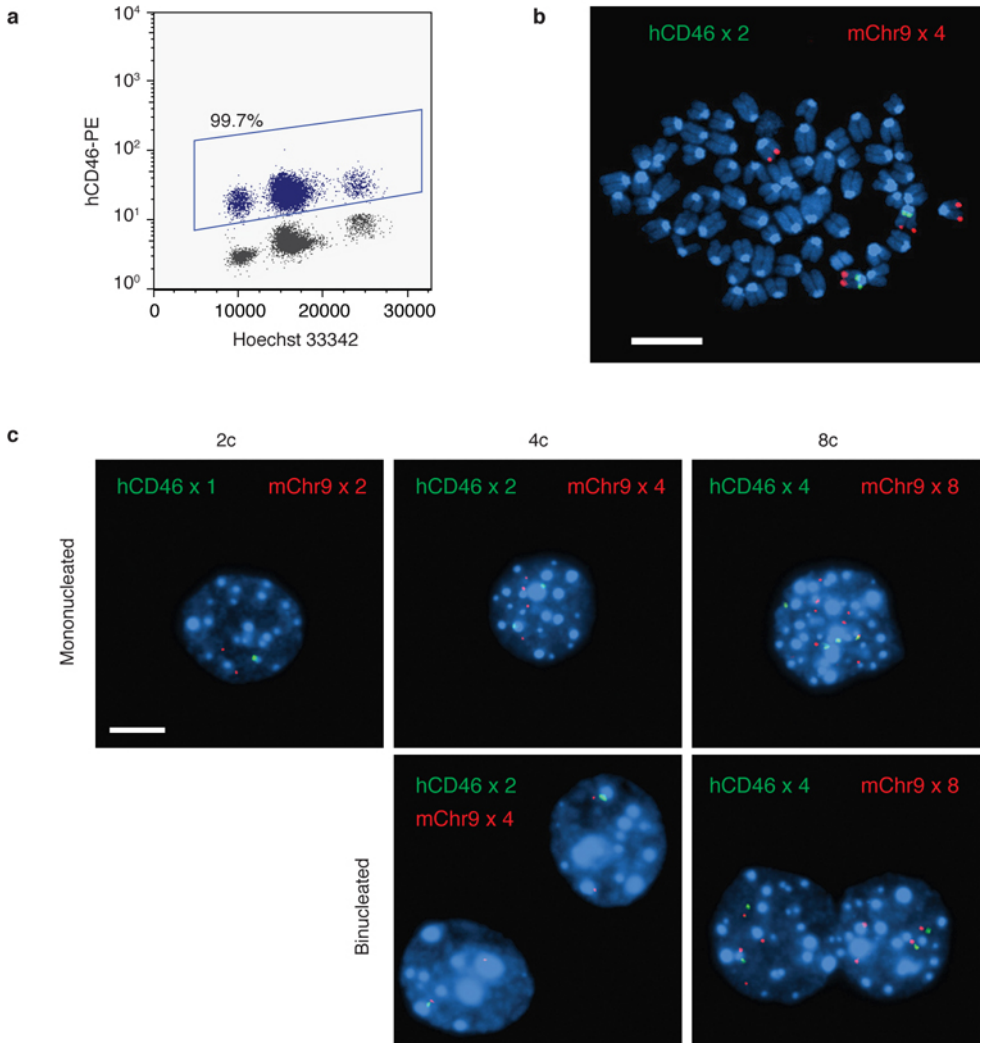

Detection of hCD46 by FACS and FISH. a, Detection of hCD46 by FACS. Hepatocytes isolated from transgenic mice hemizygous for hCD46 were loaded with Hoechst and stained a with monoclonal antibody against hCD46. FACS analysis shows nearly all hepatocytes (2c, 4c and 8c) were hCD46+ (blue). As expected, hepatocytes from wild-type mice were hCD46- (grey). **b, c,** Detection of hCD46 by FISH. Hepatocytes isolated from transgenic mice hemizygous for hCD46 were hybridized with fluorescent labeled BAC probes against hCD46 (green) and mChr9 (red). The red signal hybridizes to the telomeric end of mChr9, and the green hCD46 signal hybridizes to the centromeric end of mChr9 (**b**). Metaphase chromosomes from a tetraploid hepatocyte contained 4 signals corresponding to mChr9 and 2 signals corresponding to hCD46. Only 67 chromosomes are shown; the additional 13 chromosomes were out of the field-of-view. Signals for mChr9 and hCD46 were also detected in interphase nuclei (**c**). Diploid hepatocytes contained a single nucleus (hCD46 x 1 and mChr9 x 2). Tetraploid hepatocytes were either mononucleated (hCD46 x 2 and mChr9 x 4) or binucleated (with each nucleus containing hCD46 x 1 and mChr9 x 2). Octaploid hepatocytes were either mononucleated (hCD46 x 4 and mChr9 x 8) or binucleated (with each nucleus containing hCD46 x 2 and mChr9 x 4). Scale bars are 10 µm.

Duncan et al., Supplementary Fig. 8

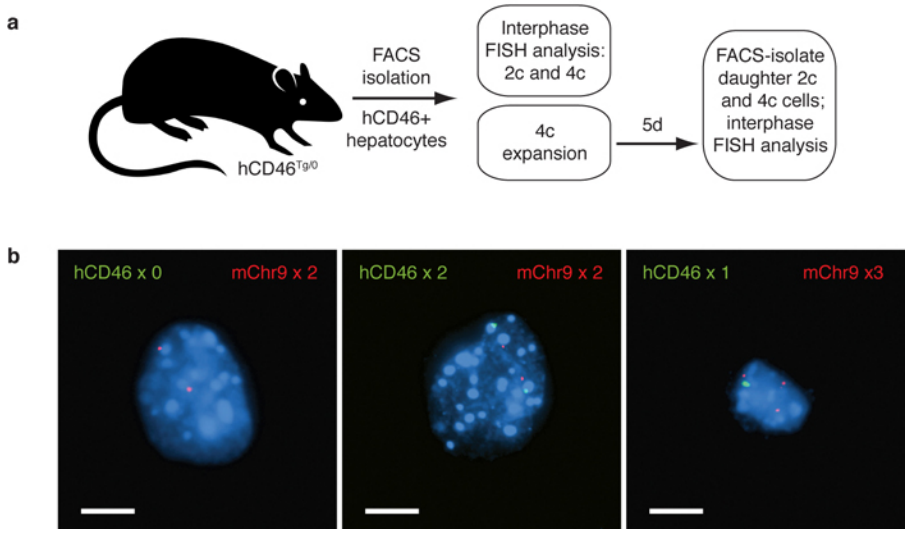

Unequal chromosome segregation during polyploid hepatocyte mitosis *in vitro.* a, Experimental design for analysis of chromosome segregation by proliferating hepatocytes. Defined ploidy populations were isolated from mice hemizygous for hCD46. After expansion of 4c hCD46+ hepatocytes for 5d, daughters with 2c and 4c content were FACS-isolated. FISH analysis was performed on the following 4 populations: freshly-isolated 2c, freshly-isolated 4c and cultured 4c (including daughter cells with 2c and 4c DNA content). Interphase nuclei were hybridized with fluorescent BAC probes recognizing hCD46 and mChr9, and the number of signals per nucleus quantified. **b,** Cultured 4c hepatocytes (2c daughters) contained atypical numbers of hCD46 (0-2) and/or mChr9 (1-3). Representative images of nuclei (blue) hybridized with probes to hCD46 (green) and mChr9 (red) are shown. Scale bars are 10 μm.

Duncan et al., Supplementary Fig. 9

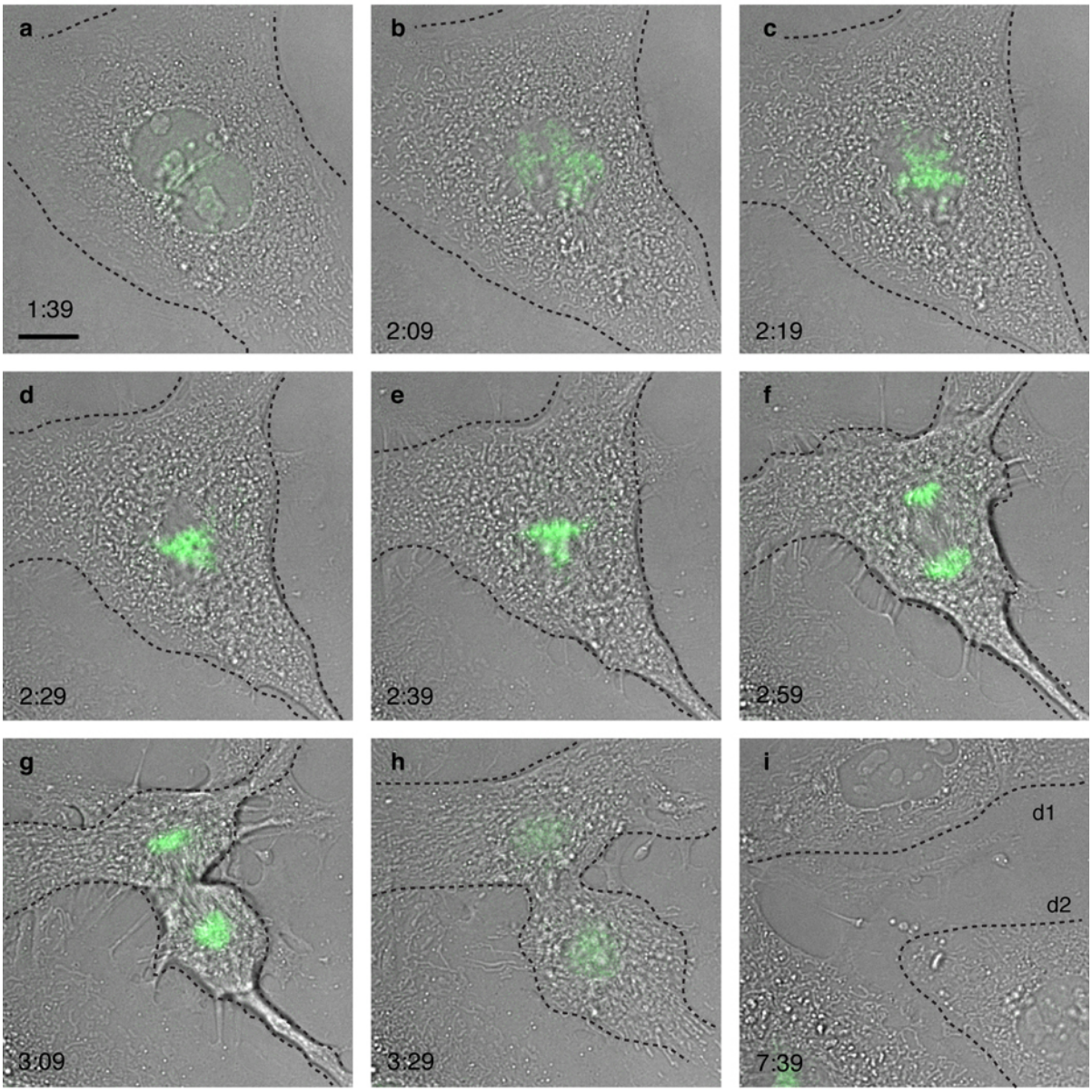

Bipolar division of 4c hepatocyte with successful cytokinesis. Time-lapse images (from Supplementary Movie 1) of a single binucleated tetraploid hepatocyte (**a**) in multiple stages of mitosis. Following chromosome condensation (**b**), chromosome alignment occurred along multiple axes (**c-e**), consistent with multipolar spindle formation. Anaphase (**f**, **g**) and telophase (**h**) proceeded in a bipolar fashion. Cytokinesis produced 2 daughter cells, d1 and d2 (**i**). Cell division was tracked with DIC (for cell structures) and Hoechst (for nuclei, pseudocolored green). Cell boundaries are marked. Scale bar is 10 μm. Time (hours : minutes) is indicated.

Duncan et al., Supplementary Fig. 10

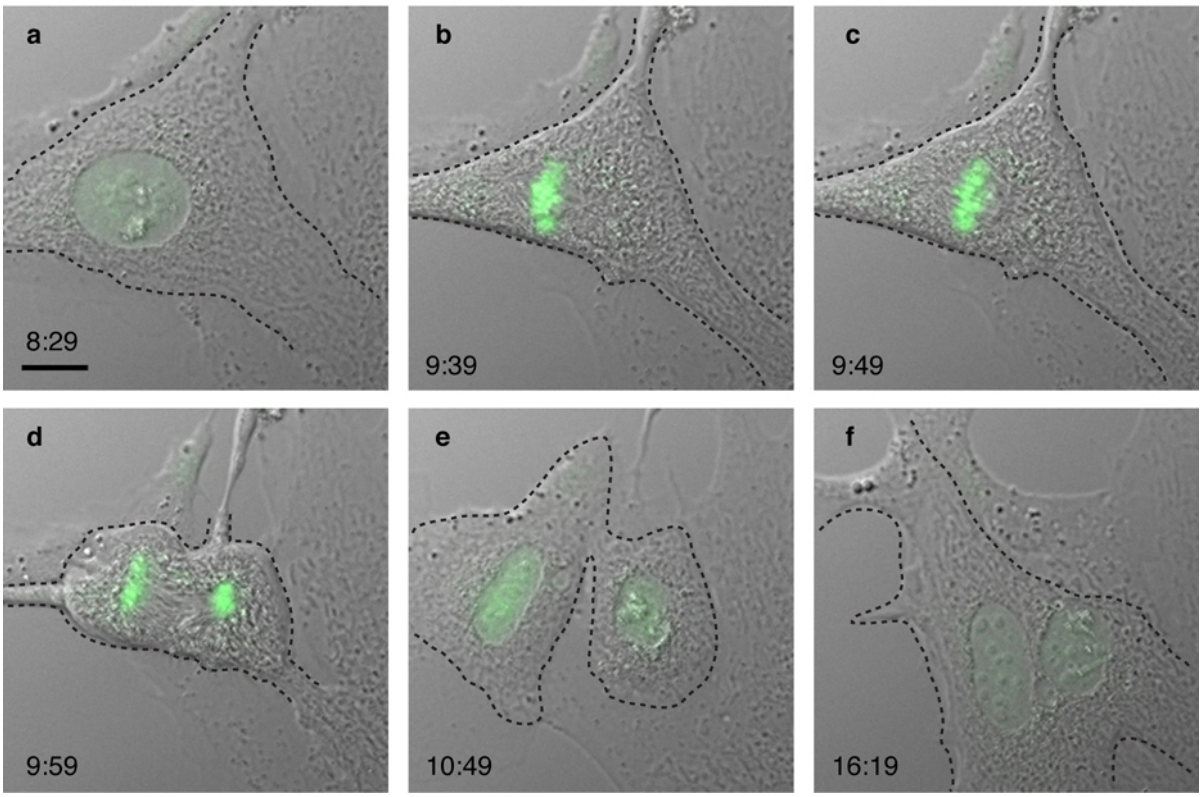

Bipolar division of 4c hepatocyte with failed cytokinesis. Time-lapse images (from Supplementary Movie 2) of a single mononucleated tetraploid hepatocyte (**a**) in multiple stages of mitosis, including metaphase (**b**, **c**) and late anaphase/early telophase (**d**). Cytokinesis fails (**e**), producing a binucleated octaploid hepatocyte (**f**). Cell division was tracked with DIC (for cell structures) and Hoechst 33342 (for nuclei, pseudocolored green). Cell boundaries are marked. Scale bar is 10 μm. Time (hours : minutes) is indicated.

Duncan et al., Supplementary Fig. 11

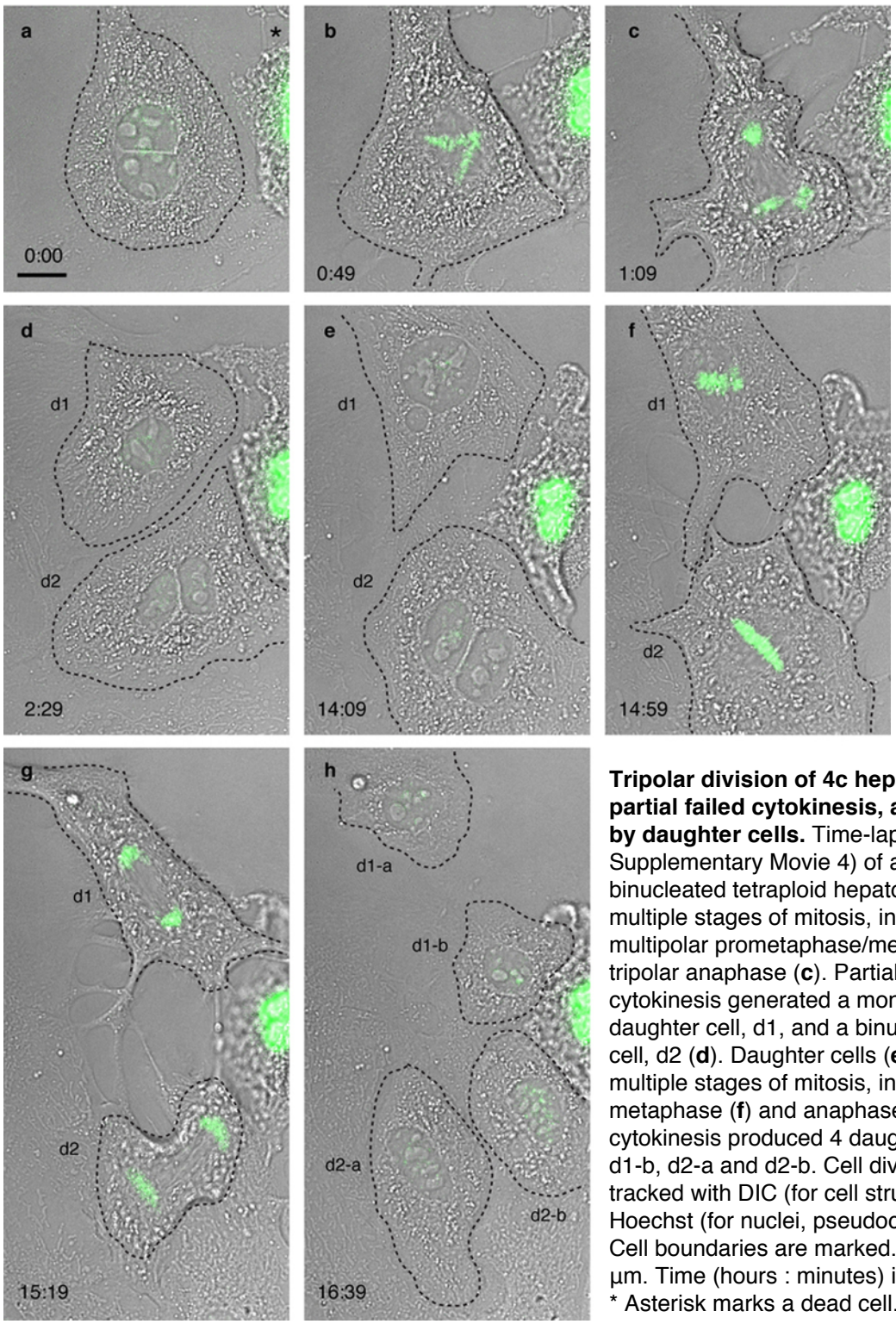

Tripolar division of 4c hepatocyte with partial failed cytokinesis, and cell division by daughter cells. Time-lapse images (from Supplementary Movie 4) of a single binucleated tetraploid hepatocyte (**a**) in multiple stages of mitosis, including multipolar prometaphase/metaphase (**b**) and tripolar anaphase (**c**). Partial failed cytokinesis generated a mononucleated daughter cell, d1, and a binucleated daughter cell, d2 (**d**). Daughter cells (**e**) are shown in multiple stages of mitosis, including metaphase (**f**) and anaphase (**g**). Successful cytokinesis produced 4 daughter cells, d1-a, d1-b, d2-a and d2-b. Cell divisions were tracked with DIC (for cell structures) and Hoechst (for nuclei, pseudocolored green). Cell boundaries are marked. Scale bar is 10 µm. Time (hours : minutes) is indicated.
* Asterisk marks a dead cell.

Duncan et al., Supplementary Fig. 12

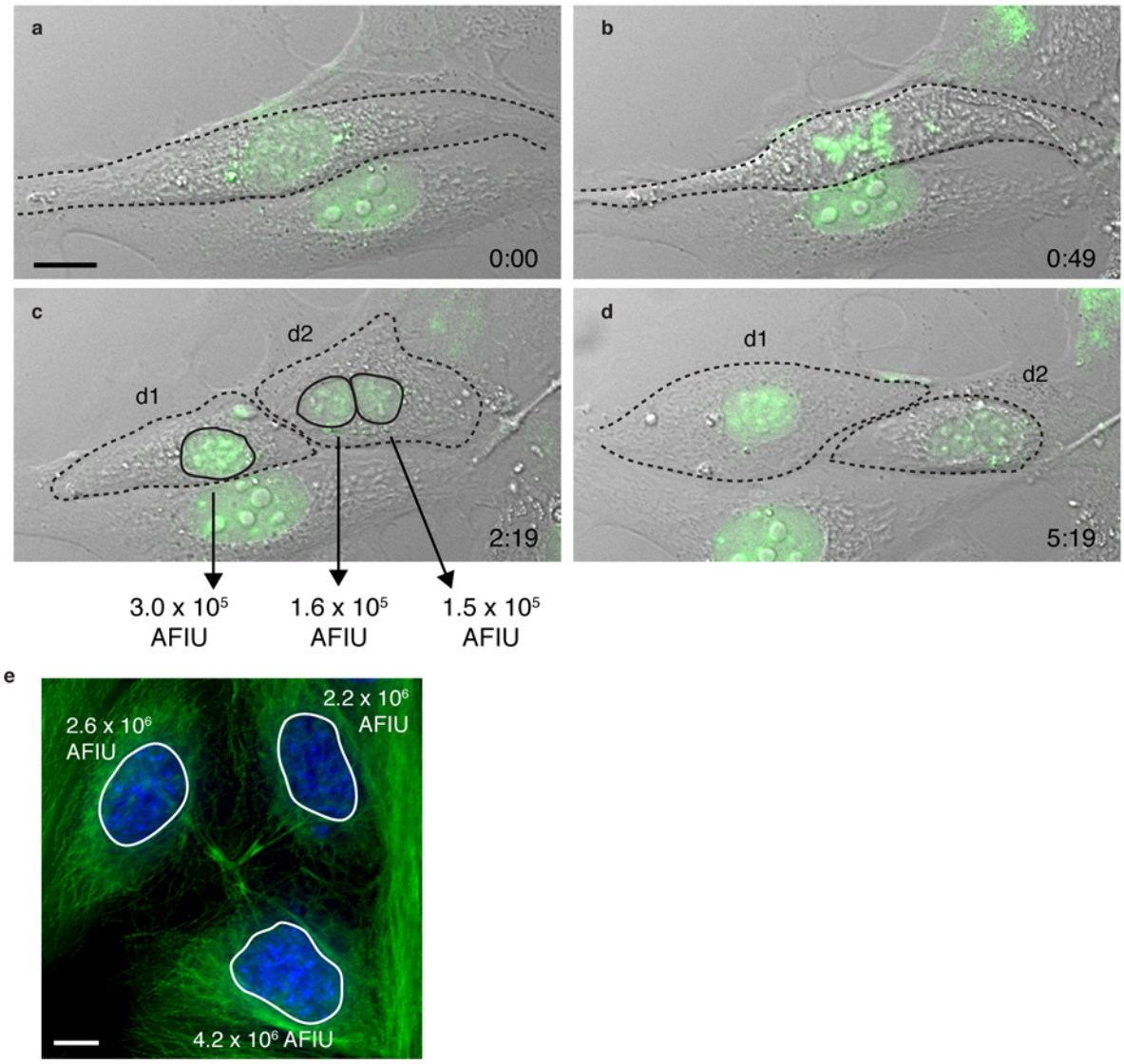

Nuclear content segregates to 3 daughter nuclei (in a 4:2:2 ratio) during tripolar mitosis. The generation of healthy, mitotically-active cells from tripolar hepatocyte mitoses was surprising. If chromosomes segregated evenly among the 3 daughter nuclei, massively aneuploid cells would result. To understand nuclear segregation in tripolar divisions, Hoechst signal in daughter nuclei was quantified. **a-d,** Time-lapse images of a single mononucleated tetraploid hepatocyte (**a**) in multiple stages of mitosis, including multipolar prometaphase/metaphase (**b**). Partial failed cytokinesis generated a mononucleated daughter cell, d1, and a binucleated daughter cell, d2 (**c**, **d**). The intensity of Hoechst fluorescence signal in each nucleus (indicated with solid lines) was determined in Artificial Fluorescence Intensity Units (AFIU) (**c**). Mitoses were tracked with DIC (for cell structures) and Hoechst (for nuclei, pseudocolored green). Cell boundaries are marked. Scale bar is 10 µm. Time (hours : minutes) is indicated. **e,** Fixed image of tetraploid hepatocyte in tripolar telophase stained with Hoechst (blue) to visualize nuclei and alpha tubulin (green) to visualize microtubules. The intensity of Hoechst fluorescence signal was determined for each nucleus (indicated with solid lines). Scale bar is 10 µm. Thus, following tripolar mitosis by tetraploid hepatocytes, nuclear content frequently segregated in a 4:2:2 ratio, which is consistent with 1 tetraploid daughter nucleus and 2 diploid daughter nuclei.

Duncan et al., Supplementary Fig. 13

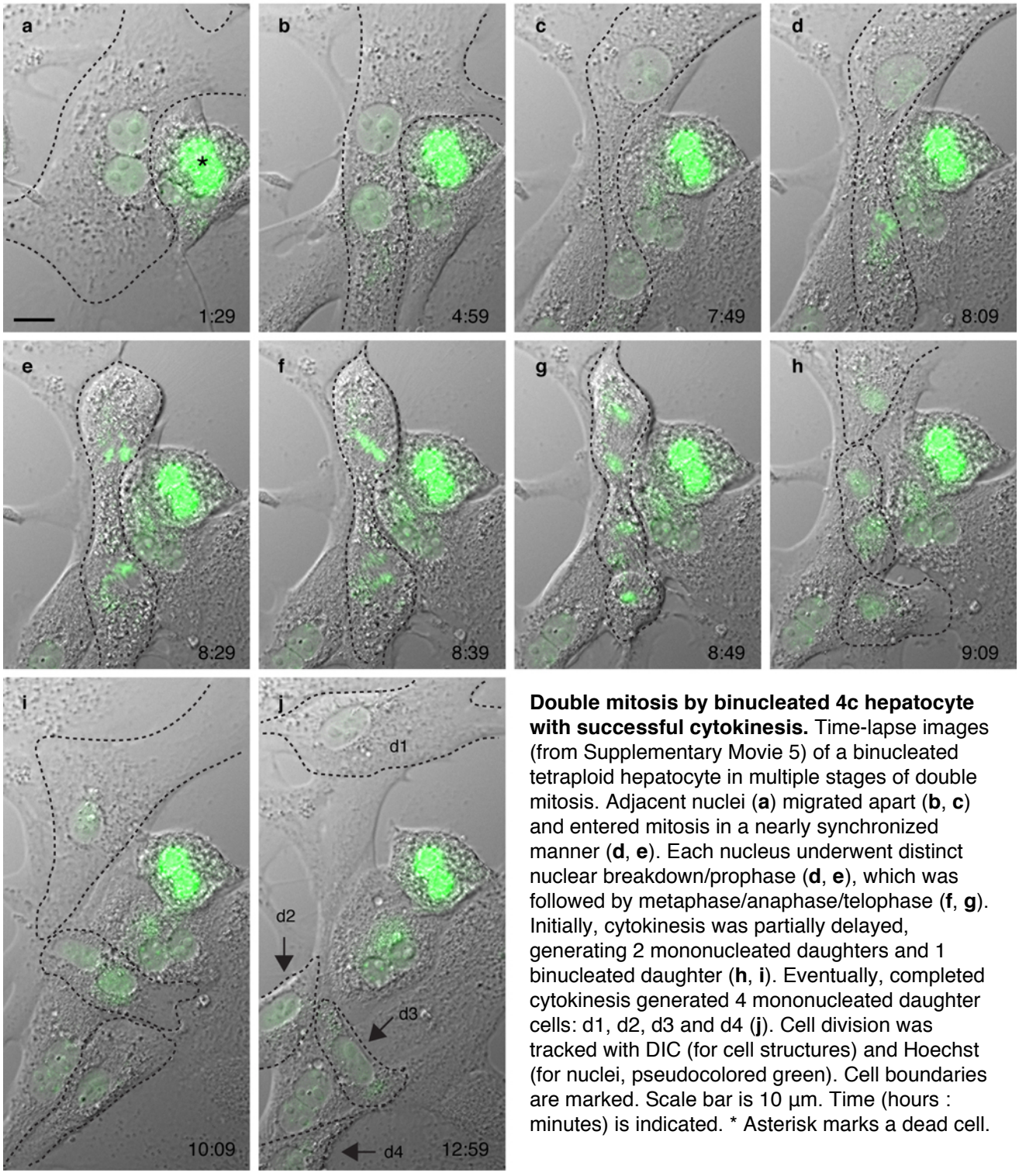

Double mitosis by binucleated 4c hepatocyte with successful cytokinesis. Time-lapse images (from Supplementary Movie 5) of a binucleated tetraploid hepatocyte in multiple stages of double mitosis. Adjacent nuclei (**a**) migrated apart (**b**, **c**) and entered mitosis in a nearly synchronized manner (**d**, **e**). Each nucleus underwent distinct nuclear breakdown/prophase (**d**, **e**), which was followed by metaphase/anaphase/telophase (**f**, **g**). Initially, cytokinesis was partially delayed, generating 2 mononucleated daughters and 1 binucleated daughter (**h**, **i**). Eventually, completed cytokinesis generated 4 mononucleated daughter cells: d1, d2, d3 and d4 (**j**). Cell division was tracked with DIC (for cell structures) and Hoechst (for nuclei, pseudocolored green). Cell boundaries are marked. Scale bar is 10 μm. Time (hours : minutes) is indicated. * Asterisk marks a dead cell.

Duncan et al., Supplementary Fig. 14

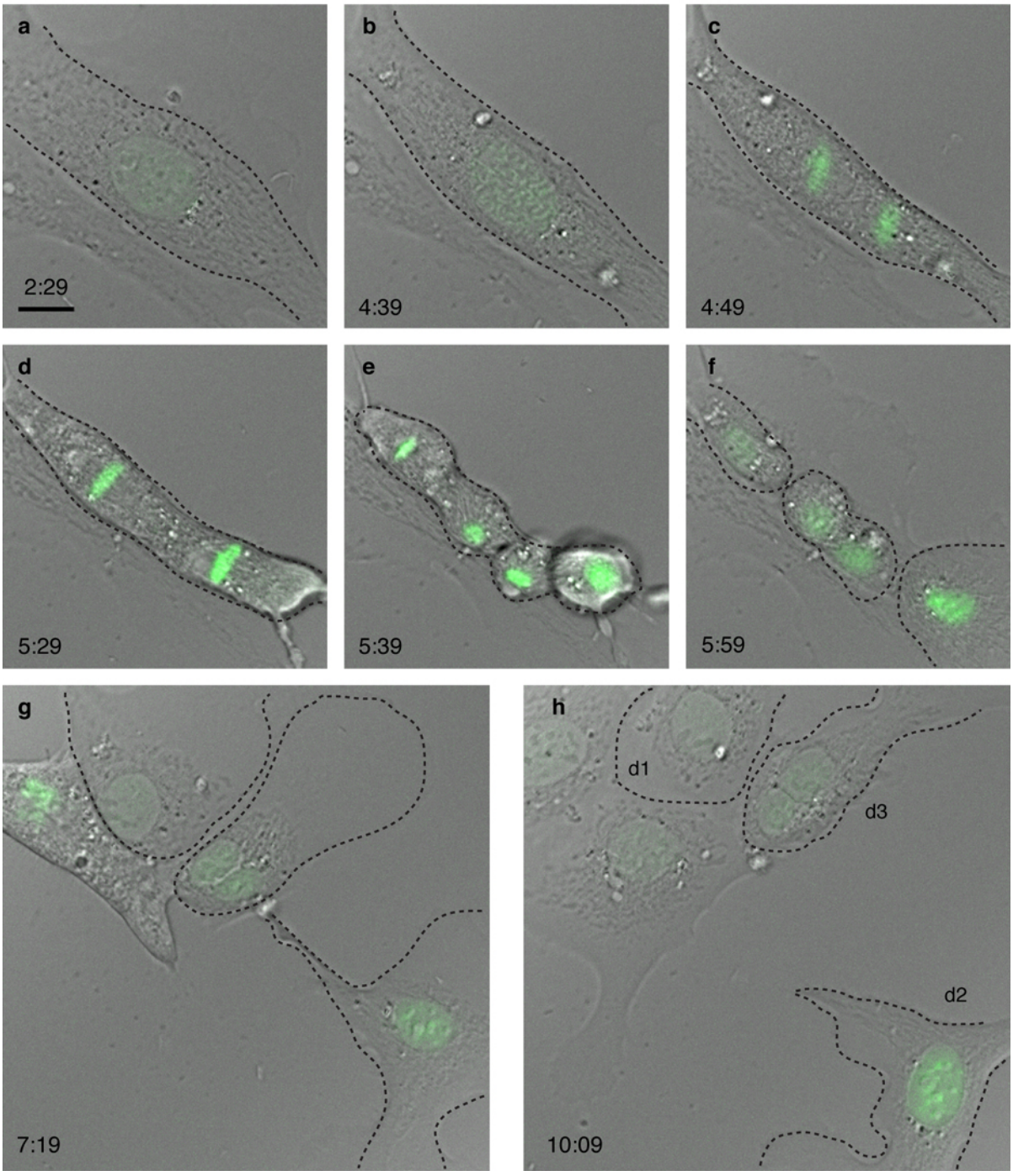

Double mitosis by mononucleated 4c hepatocyte with successful cytokinesis. Time-lapse images (from Supplementary Movie 6) of a mononucleated tetraploid hepatocyte (**a**) in multiple stages of double mitosis. Following nuclear breakdown (**b**), 2 discrete metaphase plates emerged (**c**, **d**) that underwent simultaneous anaphase (**e**) to generate 4 distinct nuclei (**f**). Partial failed cytokinesis produced 2 mononucleated daughters (d1 and d2) and 1 binucleated daughter (d3) (**g**, **h**). Cell division was tracked with DIC (for cell structures) and Hoechst (for nuclei, pseudocolored green). Cell boundaries are marked. Scale bar is 10 μm. Time (hours : minutes) is indicated.